

A New Approach for Shell Form Finding combining Numerical and Physical Design Tools

D. Weiss¹ and S. Adriaenssens^{1,2}

**¹Department of Civil and Environmental Engineering
Princeton University, Princeton NJ, United States of America**

²MEMC, VUB, Brussels, Belgium

Abstract

This paper presents a new design methodology that uses physical hanging plaster models and digital scanning techniques to appraise thin shell shapes in the preliminary design phase of a building project. The paper is divided into three parts. The first part gives an overview of the use of physical models in the development of structurally efficient shell shapes. By discussing the work of Wren, Poleni, Gaudi (i.e. hanging chains and hanging net model), Ramaswamy (i.e. hanging textile formwork), Isler (i.e. polyester resin membrane model) and Belles (i.e. models based on homeostasis), we illustrate the advantages and shortcomings of the presented physical methods and suggest how these disadvantages could be overcome. The second part introduces the new design exploration methodology that consists of three phases: Phase i) the physical hanging plaster model making, Phase ii) the digitizing of the physically form found surface, and Phase iii) the appraisal of the shell surface in terms of stresses, deflections and buckling using commercially available finite element software SAP 2000. In part 3 the paper concludes, by discussing the successfulness of the presented methodology (most specifically in the context of shell shape design exploration) and makes suggestions for other domains of application such as pre-stressed technical textile systems.

Keywords: thin shell, form finding, digitization, finite element

1 Introduction: the tradition of physical form finding for dome and shell shapes

The development of thin shell forms has allowed engineers to efficiently realize 20-30m unobstructed spans with a thickness of no more than 90mm. Traditional thin-shell design takes advantage of the compression properties of concrete in shapes designed to experience compression forces solely. This shell shape, the curved surface under which the forces are most economically transferred to the ground

supports, is the basis for their efficiency. Hanging models are at the core of the development of thin-shell forms. Heinz Isler (1926-2009), considered to have done the most thorough experimentation with hanging models stated that

“Physical models are indispensable for insights into the behavior and appearance of new shells and absolutely should not be ignored” [1].

The use of physical models has allowed engineers to fully explore the concept of form finding, and has paved the inroads of structural development with unique and essential innovations. Isler deemed the freedom of innovation allowed by physical model making “unrestricted exploration”.

It is important to note that models are still widely relevant to the present day thin-shell design process. While software has been developed to simulate the physical modelling process and forms of idealized hanging surfaces under specific load conditions, there are advantages to physical form finding. Physical form finding provides a range of design experimentation not attainable using software, to better allow for understanding between force and form and the potential for new avenues of form exploration. Educationally the process also allows for quick interactive manipulation without having decipher the working of commercial black box software. Also no real commercial software designed specifically for shell form finding is currently on the market.

The Barcelona based architect, Antonio Gaudi (1852-1926), was instrumental in the development of model experimentation. But the beginnings of hanging models can be traced even further back to Robert Hooke (1635-1703), who made the observation, *“As hangs the flexible line, so but inverted will stand the rigid arch”*. Hooke’s idea led directly to the use of hanging models, a design tool that Gaudi went to great lengths to develop as a design rather than analysis tool. Using a constant interaction between the graphic statics methods and physical models, Gaudi’s 3D hanging chain models were a solution to visualize calculations, and to easily be able to alter them [2]. Loads were suspended on hanging cables, developing tension-only forces. Inverting the form yields a new systems that is identical to the tensile system except for that compression rather than tension forces are developed.[3]. Eliciting and expounding upon the same principles that Gaudi’s hanging chain models used, engineers began using hanging models to explore thin-shell forms in the mid-1900s. Isler is one of a great many engineers to explore form through physical models, such as the mathematician Giovanni Poleni (1683-1761), famous for his modelling of catenary domes (e.g. Saint-Peter’s Dome, Rome) in the 1700s, Ramaswamy, who worked with hanging textile formwork, and Belles, who explored compression only shell forms by working with a homeostasis process. Especially through the efforts of Isler, the use of models became widespread. The hanging cloth assumes a curved shape under the single-load self-weight of the plaster, hanging only in tension while minimizing the bending part of strain energy [4].

The downfalls of the idealization of physical models are immensely important, and were apparent to no one more than Isler himself. The form can be affected by the size and shape of the undeformed original piece of material. Wrinkles, folds,

and a non-uniform application of plaster can further affect the form [4]. Isler recognized the limits of application in regard to span, thickness, and free edges in his own papers [1]. Isler stated that

“His conceptual models were only the first stage in the design process of thin-shells, and that these were followed by loading tests on small-scale models in the laboratory and long-term monitoring of built examples at full-scale” [5].

2 Thin shell design exploration methodology

2.1 Physical form finding by building a hanging plaster model

The hanging models in this study are made using fine-meshed cheesecloth, a lightweight material woven from individual strands of fibers. The pattern is a standard warp and weft pattern, where the warp threads are woven alternatively over and under the weft strands, which are held straight and parallel to each other, set orthogonal to the warp strands.

This pliability and fluidity afforded by the warp and weft proved both useful and difficult to work with. Such a material is great for experimenting with different forms and conditions. However, the pliability also results in a certain level of imperfection and inconsistency from the intended shape or uniformity, which manifested itself in the final results of the models. The individual strands can be pulled apart and stretched, altering and transforming the shape of the cloth and the orientation of the woven grid. For example, ripples and warping were common in the many models that were made and resulted in lopsided models, asymmetric, skewed in one direction by the irregularities of the fabric..

The ply of the mesh necessitated careful consideration as well. Preliminary models were made with single-ply, double-ply, and quadruple-ply cloth to see which one formed more consistent forms. Using a quadruple ply mesh resulted in a cloth that was too thick to cohesively set under the self-weight of the plaster. Using a double-ply system alleviated many of these problems, allowing for much smoother curves and a much more cohesive settling, while still allowing for a finer mesh (Figure 1).

Plaster of Paris is used as a solidifying agent, the self-weight of which determines the form of the final model. The Plaster of Paris used in these experiments was a calcium sulfate hemihydrate, with the notation $\text{CaSO}_4, \frac{1}{2} \text{H}_2\text{O}$. The Plaster of Paris requires a 2:1 plaster to water ratio with cold water. For a baseboard, treated perforated hardwood is used, the circular perforations measuring out a grid with spacing of exactly 1 inch between each hole. This grid ensures uniformity and consistency among models in regards to the placement of supports. The baseboard material used has thickness of $\frac{3}{8}$ inches, and should be cut into squares so that a grid of holes of at least 7 x 7 is on each board. Pliable yet durable string is used, cut into pieces of roughly 2 feet in length. The precision of the length is not crucial, nor the material, because the strings will be threaded through the baseboard and used only to pull the cloth up from the plaster and fasten it in position. The string should

be able to hold secure knots, and should be thin enough to fit through the grid of the cheesecloth, yet thick enough to be readily handled and tied.

Once this setup is entirely in place, the plaster is prepared by mixing 1 cup of Plaster of Paris with a half cup of water in a separate container. The plaster is thoroughly mixed, eliminating clumps entirely. Once the plaster is mixed, it is immediately poured into a shallow dish, such as a plastic plate or a disposable foil casserole dish or paint tray. The mixture is stirred once more ensuring that it is uniformly liquid. Once the plaster is mixed adequately, the cheesecloth of one model is entirely submersed in the plaster, keeping the cloth as flat as possible. The plaster is smoothed over the cheesecloth with the dowel or spreading knife, making sure that the cheesecloth is entirely coated in plaster. The cheesecloth is then extracted from the plaster by lifting the baseboard, so that the cheesecloth rises out of the plaster attached to the baseboard by the four strings. The excess plaster is allowed to drip back into the dish, and then the model is hung upside down in the previously prepared drying space (Figure 1). The baseboard should be supported on its edges on the two supports, one on each side, so that the 6 x 6 grid of the cheesecloth is entirely in between the two supports. The cheesecloth is then lifted by pulling the two knots of the strings so that each of the four knots at the corners of the cheesecloth is touching the baseboard, but not pulled through the hole. The strings are tied so that the model is secured in this position, allowing the cheesecloth to drape from each of the four corners and form the shell shape under the self-weight of the plaster. The board is secured so that it does not fall in between the supports, and tapped occasionally to ensure that the cheesecloth is fully hanging, also allowing for the excess plaster to drip off the apex of the curve. The model(s) are left in this position until the plaster is dry and the form solidified. Once this has happened, it is safe to invert the models and set them down on their baseboards, so that the inverted shell is sitting completely in compression (Figure 1).

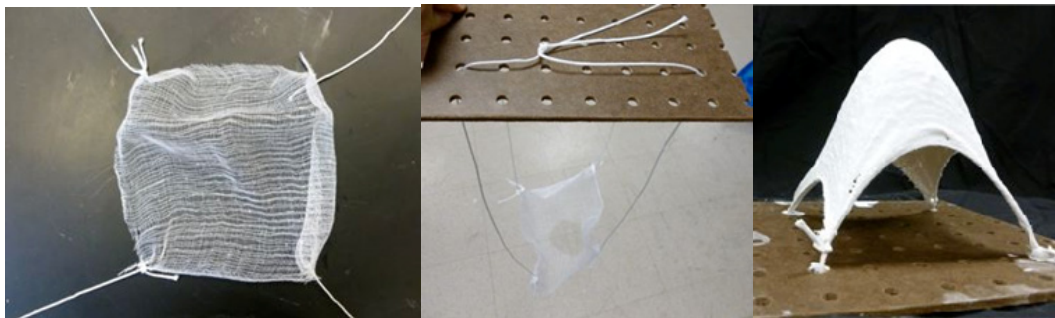


Figure 1: Cheesecloth, drying while hanging (tension) and standing in compression.

In an effort to understand the material and the process better, and to explore the potential of this type of model, a number of variations (height, edge conditions, ply, ribbing, number of supports, apertures, orientation warp and weft direction and model size) were explored. These all have different yet very real implications on the actualization of these models into full size shells but are outside the scope of this paper. Mathematically, the idealized form assumed by a hanging chain under uniform self weight (see Figure 2) can be found by the catenary equation, which is

directed primarily by the hyperbolic cosine function: $y = a \cosh\left(\frac{x}{a}\right)$. A regression was performed on 3 of the most normalized model silhouettes to examine the congruency of these plaster and cheesecloth models in light of the mathematical expectations. Two regressions were performed on standard base 6 x 6 inch models, and one on a large 9 x 9 inch model. To perform a regression, it is first necessary to obtain profiles of the models, taken from a properly aligned perspective that allows for the symmetry of the profile to be captured without a skewed perspective. A standard digital camera was used, and the pictures printed out in real size. Standardized vertical line work extending from a horizontal base line tangential to the apex of the model was drawn onto the pictures, the lines spaced at exactly 1 centimeter apart. This constituted the x-axis of the overlaid Cartesian coordinate system. Centering the drawings so that the center (0,0) point of the coordinate was at the apex of the picture, the vertical height of the model was measured to an accuracy of 1 mm (Figure 2).

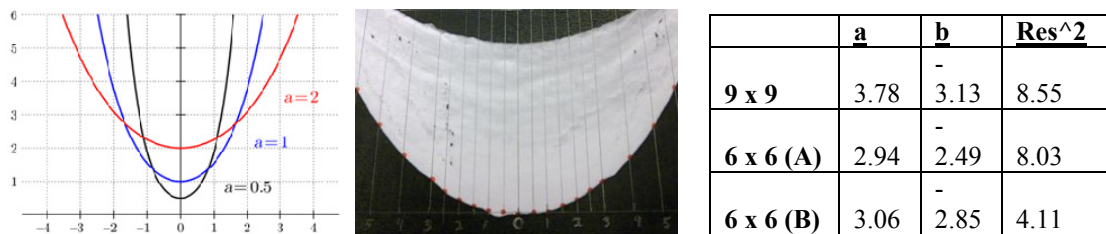


Figure 2: Catenary equation plotted, Elevation physical model with overlaid Cartesian Coordinates to compute (x,y) values, Regression results of Fitted Catenary equations.

For the standard base models, these values are taken from a range of -6 to 6 cm in the x-axis direction, with extra measurements taken at -1.5, -.5, .5, and 1.5 cm to increase the accuracy around the apex. For the 9 x 9 inch model, measurements were taken from -7 cm to 7 cm in the x-axis direction, with extra measurements taken at -2.5, -1.5, -.5, .5, 1.5, and 2.5 cm. The regression was fitted using the catenary equation and adding a y-intercept constant (b) so that the equation is $y = a \cosh\left(\frac{x}{a}\right) + b$. Both (a) and (b) are manipulated until the square of the residuals was minimized as shown in Figure 2. These results confirm the consistency between the physical form found shapes and the analytically expected shape. The discrepancies for the wider data points is most likely due to the uneven distribution of the self-weight load of the plaster over the cheesecloth. As the cheesecloth is hung to dry, gravity pulls the density of the plaster to a central concentration on a radial gradient, that leaves the center of the shape mathematically predictable, but levels out the sides of the form close to the supports. The constraint of the warp and weft of the fabric might also play a role in the deviation in the outer range of the curve from the catenary formula. But overall it is very beneficial to observe the reaction of the models in relation to the mathematical models for tensile hanging behavior.

2.2 Digitization of the physical form found shell shape

2.2.1 The digital workflow

The ability to digitize physical models is new to the exploration of form in thin-shell design. Digitization in this context refers to the process of converting the physical model to a digital model. The goal of this digitization is to obtain structural analysis results from a finite element analysis of the digital replica of the physical model. The physical model was first made and then digitally scanned with the handheld digital scanning wand. The model was prepared so that the scanner could most easily read the surface of the model. The surface was sanded with fine-grain sandpaper, smoothing over bumps and ridges that came from the physical modelling process. Any small gaps or holes in the plaster were filled in and smoothed over with a thin coat of plaster, to proffer as uniformly smooth a surface as possible for scanning. The 3D scanning wand is used to initiate the process of digitization. The scanner transmits data in the form of 3-D relative singular points to the receiving program (in this case) FastSCAN, that accompanies the 3D surface digitizer Polhemus. After the model is digitally rendered as accurately as possible, the number of points comprising the digital rendering was on the order of tens of thousands.

After the scanning is complete, the digital model must be “cleaned up” to better facilitate the analysis process. The level of sensitivity in the scanner is too low to procure a flawless digital model. Extra data points where the sensor picked up parts of the table surface, gaps in the data points where the scanner might have missed small sections of the model, and slight incongruence in the flushing of different sweeps, are common imperfections. The final product of this section, however, is a triangular mesh that is extruded from the data points, where each data point is a node, triangularly connected to the nodes around it. This mesh can be exported as a .dxf file to be further manipulated in AutoCAD, a program aiding in the digital manipulation of structural design.

AutoCAD provides the opportunity to further clean up the mesh, and to properly scale the table size model to a 20-30m span system. Extraneous points can be deleted, obtrusions from the mesh can be corrected by dragging points in line with the mesh, and a standard unit of measurement established. From this point, the .dxf file is imported into SAP2000 and attributed a thin shell element. SAP is a program that allows for FE analysis on the imported digital mesh of the physical model.

2.2.2 Three dimensional scanning

The Polhemus FastSCAN Cobra 3-Dimensional Laser Scanner boasts the first exploration into the realm of handheld 3-Dimensional scanners. The wand emits a horizontal red laser scan that, when swept over the physical model in a manner similar to spray painting, relays data in the form of dots to the receiving FastSCAN program (Figure 3). The wand is connected to the main functional Processing Unit of the system, which is connected by way of a USB cable to a computer. The transmitter, a cube also attached to the Processing Unit, is placed as close to the

model being scanned and as far away from the hard drive as is feasible, to avoid interference. This transmitter acts as a reference point for the wand, so that the relative spatial configuration of the model can be maintained as the data is transmitted. As the wand scans the model, the relative location of each point is determined in reference to this transmitter, allowing for an accurate digital recreation of the model. The data is automatically imported into a program entitled FastSCAN. This program allows one to delete extraneous points, generate basic surfaces, and smooth and manipulate these meshes.



Figure 3: FastSCAN wand, laser and Wand, transmitter, and Processing Unit (from top to bottom)

Figure 4 shows the data displayed as individual dots compiled during the scanning sweeps. The purpose of scanning at this stage is to procure a mesh that can be exported and analyzed. This mesh can be procured by simply generating a basic surface, editing the *Decimation* value to manipulate the number of points and triangles in the mesh, extrapolated from the surface point data recorded by the wand. The mesh was reduced to comprise 800 triangular elements at a decimation level of 8.00. The smoothing level was set to 3.50 in the generation of the surface, smoothing over the deformities caused by the scanning without diminishing the integrity of the original shape. The data as a mesh and as a solid surface are shown in Figure 4. This level of subdivision ensured accuracy in the sensitivity of the mesh, without overloading the analysis with unnecessary data and an overlarge file size.

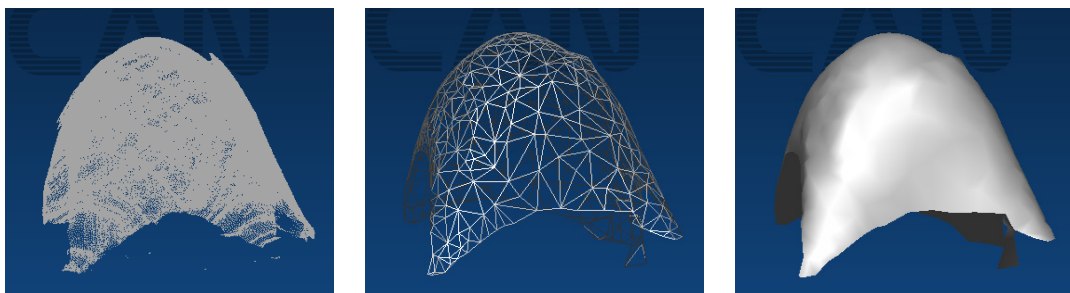


Figure 4: Data points and sweeps, Mesh surface and Solid generated surface

With the mesh completed and affected to the desired level of complexity, the file is exported as a .dxf file into AutoCAD, where steps are taken to properly scale the model. The imported model was scaled to be 20 meters in length along each edge of the model. This scaling was chosen as a standard due to the average span of shells

being in the range of 20-30 meters in length, and Isler's calculations often initially done on structures 20 meters in length [5]. Further changes can be made to individual points in the mesh that are a product of the miscalculation in the scanning process.

The .dxf file, properly scaled, was then imported into SAP for the assignment of physical properties, and the performance of finite element analysis. The material, the thickness, the load conditions, and the support constraints were then defined. The specifics of the numerical analysis will be included in the next section 2.2.. This assignment of physical properties is a major area of numerical experimentation with the physical analysis. A number of manipulations were performed with material thickness and load assignment, however it is recognized that this is only a brief exploration into the capabilities of the physical models from a numerical standpoint.

2.2 Numerical Analysis of the Physical Model

2.2.1 Input data

The mesh was set as a thin shell element type upon uploading the mesh into SAP. The materiality was set to concrete with strength of 4000 psi, the resistive strength of concrete in compression already included in the program as a functional constant. An initial thickness of the thin shell was set to an initial estimate of 3 inches, 76mm, similar in depth to many of the currently existing shells (Chilton, 2000). With a span of 20 meters in length, the thickness to span ratio is equal to $.0762/20 = .00381$. Possible bending may be induced by imperfections and bumps in the form, as well as asymmetric loading. Pin joints were placed at the four corners of the model, and the dead load was given a multiplication factor of 1.2, as is the US Building Code required load coefficient. For this first analysis, only the dead load is considered.

The conditions being defined and assigned, the model is ready to run the linear analysis. Numerical results were reviewed graphically, detailing the study of different stresses taken at different depths of the shell. The digital model was first analyzed, comparing the S11 stresses, principal stresses, at both the top and bottom layer of the shell thickness. This comparison would reveal the distribution of stress throughout the section of the shell membrane, showing whether or not the shell truly works in membrane action. Similar values in each location at both the top and the bottom of the shell would reveal a uniform stress distribution (Figure 5).

While the values for each are in an extremely close range, it can be noted that the green and orange coloration are positive and negative stresses respectively. This difference in sign that occurs between the top and bottom of the shell thickness indicates that the stress throughout the depth of the shell is not uniform. There are, however, areas of the shell that indicate very uniform stress distribution throughout the shell depth, where the colors are similar in both the top and bottom view diagrams. While it must be noted that the differences of the stresses are relatively small, this opposition is unexpected, and must be attributed to incongruence of the shell form. The differences in form at the supports are large enough to produce this discrepancy.

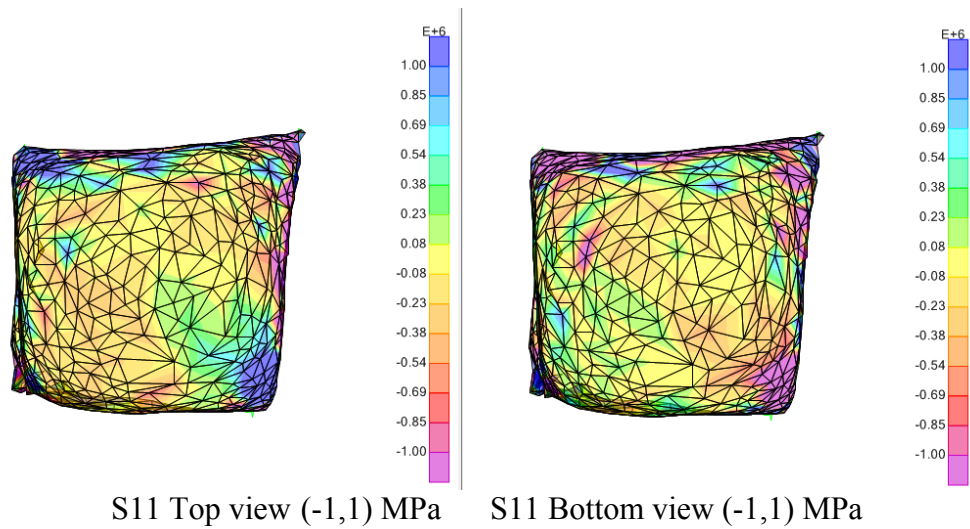


Figure 5: Principal stresses in the top and bottom surface of the shell under self weight.

Under the dead load condition, deflection was minimal and hardly visible, relative to the undeflected mesh. However, deflections were recorded in 6 points, 2 at the apex of the mesh and one at each edge, at the apex of the arches created by the edges of the material. It should be noted that significantly more deflection and stress was observed near the supports of the model, but this can largely be attributed to the non-normal form these parts of the model have taken, both from the imperfections of the physical model and the inability of the 3-Dimensional scanner to accurately read these parts of the model. As such, this analysis will be more concerned with the upper, more centralized parts of the mesh. These 6 points were determined to be the joints (excluding the mesh near the supports) at which the model would deform most. The results for vertical deflection are included in Table 1 below, both for the analysis run at 76mm of shell thickness, and for a subsequent analysis run at 51mm of shell thickness.

	Deflection (m) at t = .0762 m	Deflection (m) at t = .0508 m
top joint 140	-0.0092	-0.0121
top joint 170	-0.0099	-0.0131
side joint 426	-0.0221	-0.0309
side joint 147	-0.0426	-0.0559
side joint 178	-0.0071	-0.0088
side joint 494	-0.0008	-0.0017

Table 1 – Local deflections

The serviceably acceptable deflection for concrete structures is span/200. As such, for a span of 20 meters, acceptable deflections must be <10cm. Deflections in both analyses fulfill this requirement, as the largest value in the 51mm thickness analysis is 5.5cm deflection in the vertical direction. Generally, vertical deflection

at the top of the model was between 1 and 2cm, and increased to 3 to 7cm meters closer to the supports.

An additional analysis was performed under increased dead load, to test the capabilities of the model under extreme load conditions, and determine the amount of room for an imposed live load. Stresses experienced at this level of 10 times the dead load experienced in the first analysis, are still on the order of ~1-3 MPa at the apex of the shell, and up to 20 MPa in the sides close to the support of the shell. Under a dead load factored at 10 times the real load, the shell is still well within the allowable limit of stress for thin-shell concrete structures. With the analyses run on this digital model, it was confirmed that while the shell is working uniformly under compression, there is an uneven distribution of stress along the depth of the shell, most likely attributed to the irregularity of shape, especially towards the supports.

The final analysis of the shell is an approximation of the buckling capacity, according to the equation presented by Isler in a colloquium paper in 1982 [5]. The equation is an inexplicit “general” equation that was used by Isler more to inform than to dictate a value. The equation is as follows

$$P_{cr} = c * E * \left(\frac{t}{r} \right)^x \geq s * P_{eff} \quad (1)$$

Where

P_{cr}	critical buckling load
E	modulus of elasticity
c	modification factor, chosen to be 0.3 (Chilton 2000)
t	shell thickness =76mm
r	local radius of curvature (scaled from model)
x	power of curvature, chosen to be 2 (Chilton 2000)
s	safety factory
P_{eff}	actual load

Plugging in each of these variables into the buckling equation, P_{cr} is on the order of 27.5 MPa. This value may largely be affected by the value of c, the modification factor. Though however vague the value of the modification factor, it is interesting to affirm Isler’s buckling estimation by arriving at a value on the same order of magnitude as the allowed stress in concrete.

3 Conclusion

This paper briefly reviewed the evolution of use of physical models in the shape finding process for compression only domes and shells. Subsequently a 3 phase methodology was presented that combines physical, digital and numerical design tools to enable design exploration at a preliminary design stage. In Phase 1 a technique to make physical plaster hanging models is presented. These physical

models are digitized using a 3D Laser Scanner in Phase 2. The results of this digitisation is a triangular mesh, which is scaled to realistic proportions. This new model is then imported in a standard commercial Finite Element Package. The Finite Element Analysis shows that the stresses experienced by the shell under self weight were well within the allowable stresses of thin concrete shells, and also that the model was shown to withstand the imposed stresses under a dead load at 10 times the normal dead load while staying under the allowable stress limit. Deflections were around 10cm towards the center of the model, which is 1/10 the allowable deflection of concrete spans. While the stress distribution throughout the shell depth was inconsistent with expectations of near uniformity, the shell was acting under Maximum stresses of uniform compression, and the buckling capacity estimated by Isler's model equation was on the same order as the allowable stress of concrete. The proposed form finding methodology holds promise for both hanging and pneumatic models provided these last ones are made with sufficient level of accuracy.

References

- [1] Isler, H. "*Concrete Shells Derived from Experimental Shapes.*" Structural Engineering International, Vol. 4. No. 3. 1994.
- [2] Huerta, S. "*Structural Design in the Work of Gaudi.*" Architectural Science Review, Vol. 49. No. 4. 2006
- [3] Felicetti, P. Tang, J.W. Xie, Y.M. "*Form finding for Complex Structures Using Evolutionary Structural Optimization Method.*" Design Studies, Vol. 26. No. 1. 2005
- [4] Bletzinger, Wuchner, Daoud, Camprubi. "*Computational Methods for Form Finding and Optimization of Shells and Membranes.*" Computer Methods in Applied Mechanics and Engineering Vol. 194. Issues 30-33. 2005.
- [5] Chilton, J. "*The Engineer's Contribution to Contemporary Architecture: Heinz Isler.*" Thomas Telford Publishing, London. 2000